Appl. Phys. B 87, 311–315 (2007)
DOI: 10.1007/s00340-007-2582-1

Applied Physics B
Lasers and Optics

A. GUPTA[1,✉]
N.K. VERMA[2]
H.S. BHATTI[1]

Fast photoluminescence decay processes of doped ZnO phosphors

[1] Department of Physics, Punjabi University, Patiala, India
[2] SPMS, Thapar Institute of Engineering and Technology, Patiala, India

Received: 16 July 2006/Final version: 24 November 2006
Published online: 2 March 2007 • © Springer-Verlag 2007

ABSTRACT Lifetime measurements have been carried out for ZnO doped with killer impurities (Fe, Co or Ni) having doping concentrations 0.05 to 1.00% by weight using a pulsed UV laser (nitrogen laser) as the excitation source having a short pulse width and a high photon flux density. The high photon flux density of the laser is very useful to excite the short-lived shallow trapping states which otherwise would be impossible to excite. Fast photoluminescence emission in the microsecond time domain has been obtained due to killer impurities at room temperature. The effect of killer dopants as well as the effect of their concentrations on lifetime values has been observed. Other optical parameters such as trap depth and decay constant are also reported in the present context. Lifetime values are found to be in the microsecond time domain and a reverse trend is obtained with increase in concentration of killer impurities.

PACS 78.55.-m; 78.55.Ap; 78.66.Db; 78.66.Hf

1 Introduction

The wide band gap II–VI semiconductor compound ZnO with exciton binding energy 60 meV has potential technological and industrial applications in both short-wavelength and visible light-emitting devices [1–3]. The centers responsible for the unstructured emission bands in the green, yellow and red spectral regions are usually assumed to be due to different native defects in ZnO, such as oxygen vacancies, zinc vacancies, interstitial zinc, interstitial oxygen and antisite defects [4–7]. Until now, no clear evidence concerning the nature of the defects responsible for the origin of the luminescence has been reported in the literature. Besides the intrinsic nature of defects responsible for green, yellow and red luminescence, some authors believe that the recombination processes are due to extrinsic charge carriers, such as Li and Cu. The Cu-related emission band is known to be a LO-phonon-assisted transition with zero phonon lines, with the emission characterized by a fast exponential decay (440 ns at 1.6 K) [8–11]. Monteiro et al. [10], from the experimental observations, argued that the (Cu^{+}, h) state in crystals with less than 250 ppm copper concentration decays purely radiatively to the ground state. With extrinsic excitation, the red, Fe-related emission was observed up to 120 K. Slack and O'Meara [12] have observed that the luminescence of Fe-doped ZnS phosphors occurs over a band between 2400 cm^{-1} and 3000 cm^{-1} corresponding to zero phonon lines at 5 K. The luminescence output was reasonably independent of the iron concentration, thus indicating that iron is not a killer of its own luminescence. Many compounds exhibit a characteristic red luminescence ascribed to $^4T_1 - {}^6A_1$ transitions in the trivalent iron ion [13, 14]. Divalent cobalt has spectroscopic properties in certain compounds that allow these crystals to function as tunable vibronic solid-state lasers [15]. In other crystalline hosts, Co^{2+} serves as a saturable absorber for Q-switching of near-infrared solid-state lasers [16, 17]. Gruber et al. [17] have observed the fluorescence spectrum of divalent cobalt in zinc metaborate at 8 K between 550 nm and 900 nm. A relatively strong band was observed at 574 nm and a weak band was observed between 600 nm and 855 nm. The weaker fluorescence band represents vibronic and electronic transitions from ^2E (^2G), ^4T (^4P) mixed states to the ground $^4A_2$ (^4F) and $^4T_2$ (^4F) states, which was supposed to be due to Co^{2+} associated with a charge-absorption band, viz. ZnO–Co^{2+}. Further, they have shown that the low luminescence quantum efficiency and temperature dependence of the emission provides evidence for strong quenching of luminescence due to nonradiative relaxation processes. Recombination rates of trapped charge carriers in nanocrystalline ZnO thin films have been measured by means of time-resolved emission spectroscopy by Bauer et al. [18]. They have used a femtosecond laser to obtain the recombination rate to be 400 ps of shallowly trapped electrons with deeply trapped holes using a single photon counting technique. However, earlier Kamat and Patrick studied the emission decay of ZnO nanoparticles at room temperature and fitted the decay curves to three exponential components; the fastest component observed was 1.63 ns using a picosecond laser [19]. Time-resolved photoluminescence provides an effective nondestructive technique for studying the dynamics of impurities and lattice defects in semiconductors [20]. Bhatti et al. [21] have observed photoluminescence spectra for ZnS co-doped with Mn and Ni where three peaks at 412 nm, 433 nm and 590 nm corresponding to Ni impurity, sulphide

✉ E-mail: virgoatul@yahoo.co.in

vacancies and Mn impurity, respectively, have been obtained. A lifetime value of 28.07 ns corresponding to Ni impurity in ZnS:Mn with a nanosecond laser using a pulse excitation method has been obtained from the multiexponential decay curve.

During the present investigations, killer (Co, Fe or Ni) impurity doped ZnO semiconductor compound bulk phosphors have been synthesized and their lifetime, trap-depth and decay-constant values have been simulated by a pulse excitation method using a pulsed UV nitrogen laser having a short pulse width in nanoseconds and a high photon flux density per peak. To the best of our knowledge there is no report of the lifetime, trap-depth and decay-constant values of zinc oxide phosphors doped with killer impurities, excited by a nitrogen laser. Most of the reports discussed above and available in the literature show that impurities like Fe, Co and Ni are the killers of visible luminescence of the ZnO phosphors and deal with the luminescence either at low temperature [8–11, 17] or in the infrared region [16, 17]. However, this report deals with the successful achievement of the visible luminescence of the killer-doped ZnO phosphors at room temperature and determinations of the lifetimes of the excited states and the corresponding trap-depth values by a well-known pulse excitation method [21, 22]. The source of excitation used was a nitrogen laser having a high peak power which was responsible for excitation of killer levels from where the luminescence was observed. X-ray diffraction studies indicate no separate phase formation in doped ZnO phosphors, which may be due to low concentration of impurity.

2 Experimental

2.1 *Synthesis method*

Doped ZnO phosphors with variable concentrations of killer impurities have been synthesized in the laboratory. Doping of cobalt has been achieved using Co_3O_4 and

ZnO phosphor: impurity (%)	Lifetime values (μs) at 300 K			Trap-depth values (eV) at 300 K			Decay-constant value
	t_1	t_2	t_3	E_1	E_2	E_3	b
ZnO:Co (0.05%)	6.89	16.59	26.56	0.230	0.253	0.265	0.56
ZnO:Co (0.1%)	6.55	15.62	25.63	0.228	0.251	0.264	0.58
ZnO:Co (0.3%)	6.54	15.62	25.63	0.228	0.251	0.264	0.67
ZnO:Co (0.5%)	6.32	14.56	24.36	0.227	0.249	0.263	0.53
ZnO:Co (0.7%)	6.32	13.65	22.65	0.227	0.247	0.261	0.58
ZnO:Co (1.0%)	5.61	12.35	20.65	0.224	0.245	0.258	0.63
ZnO:Fe (0.05%)	4.89	13.69	22.56	0.221	0.248	0.261	0.55
ZnO:Fe (0.1%)	4.69	12.65	22.31	0.220	0.245	0.260	0.54
ZnO:Fe (0.3%)	4.66	12.62	21.63	0.220	0.245	0.260	0.65
ZnO:Fe (0.5%)	6.26	16.39	25.36	0.227	0.252	0.264	0.62
ZnO:Fe (0.7%)	4.32	12.35	20.31	0.218	0.245	0.258	0.56
ZnO:Fe (1.0%)	3.98	9.58	15.26	0.215	0.238	0.250	0.50
ZnO:Ni (0.05%)	9.99	16.32	26.56	0.239	0.252	0.265	0.54
ZnO:Ni (0.1%)	9.58	16.31	25.65	0.238	0.252	0.264	0.53
ZnO:Ni (0.3%)	9.56	16.31	25.36	0.238	0.252	0.264	0.52
ZnO:Ni (0.5%)	12.36	19.65	36.56	0.245	0.257	0.273	0.62
ZnO:Ni (0.7%)	8.65	15.36	24.63	0.236	0.251	0.263	0.63
ZnO:Ni (1.0%)	7.65	14.36	20.36	0.232	0.249	0.258	0.68

TABLE 1 Lifetime, trap-depth and decay-constant values for doped ZnO phosphors

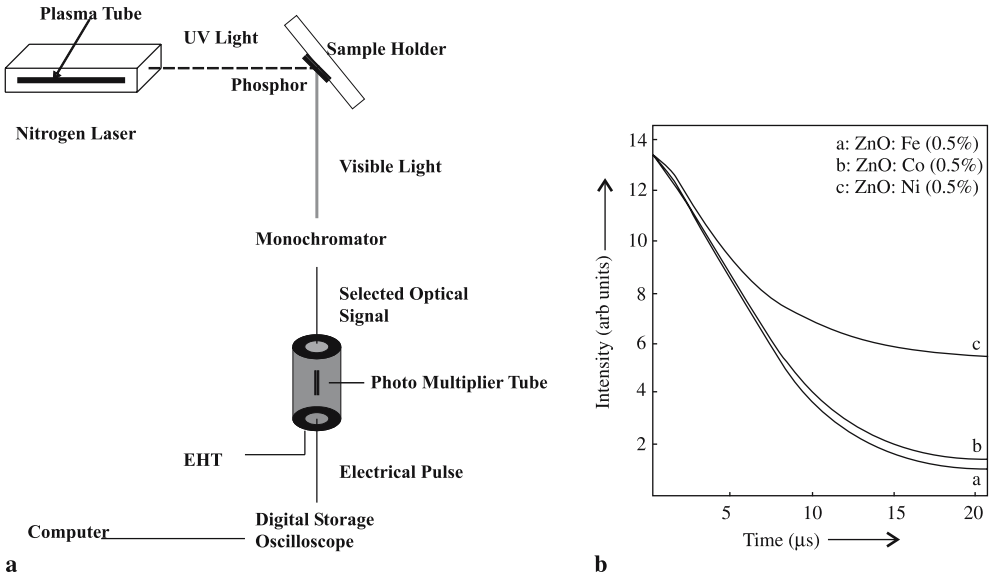

FIGURE 1 (**a**) Experimental set-up using a nitrogen laser as an excitation source. The monochromator acts as a wavelength-selective element and the photomultiplier tube as a transducer to convert the optical signal to an electrical signal. (**b**) Decay curves of laser-excited ZnO:Fe (emission wavelength = 653 nm), ZnO:Co (emission wavelength = 620 nm) and ZnO:Ni (emission wavelength = 510 nm)

ZnO by grinding them in ethanolic media for several minutes and then giving a heat treatment to them at 900 °C for two hours. A similar procedure is opted for nickel doping using nickel nitrate and zinc oxide as starting compounds. For doping iron in zinc oxide semiconductor, metal powders of Fe, lead oxide and zinc oxide have been used. After heat treatment the samples were washed with deionized water and dried in an oven at 100 °C for half an hour. The concentration of killer ions varies from 0.05% to 1.00% by weight to obtain a better insight.

2.2 *Experimental set-up for photoluminescence measurements*

The mixtures of powders were crushed into fine powder form and were then pasted in the groove of Pyrex glass (sample holder) using xylene. A high peak power, pulsed operation nitrogen laser (10 kW, 10 ns, 337.1 nm) was employed as an excitation source. Luminescence in the visible region was observed from the killer-doped ZnO phosphor. Emission was observed at an angle of 90° to the laser beam and the emission wavelength was selected by a monochromator. After selection of the emission wavelength the signal was sent to a photomultiplier tube (PMT), which acts as a transducer to convert the optical signal to an electrical signal. The electrical signal was sent to a digital storage oscilloscope coupled with a computer assembly from where decay curves were observed and finally sent to a computer for simulation purposes. Three lifetime and trap-depth values [21, 22] (using (2) and (3), respectively) have been peeled off and from the $\ln I$ vs. $\ln t$ graph decay-constant values of corresponding transitions have been calculated using (3) and reported in Table 1.

2.3 *Procedure for lifetime, trap-depth and decay-constant value measurements*

The intensity obtained from the laser-induced decay curves of ZnO phosphors is given by the following relation:

$$I = I_0 \mathrm{e}^{-pt}, \tag{1}$$

where I is the intensity of phosphorescence radiation at time t, I_0 is the intensity of the radiation at the cut-off position and the constant p is the transition probability of the corresponding radiative transition. A plot of $\ln I$ vs. t will be a straight line in the case of a single lifetime. However, in most of the cases, when one comes across the interaction of radiation with solids, there are trapping levels at many different depths leading to multiple trap depths giving hyperbolic decay curves. The decay curves have been peeled off into three components by the peeling off method of Bube using computer simulation [21, 22]. Transitions from the various traps corresponding to transition probability values [23, 24] are obtained from the following relation:

$$p = S \mathrm{e}^{-E/kT}, \tag{2}$$

where E is the energy of the level in the forbidden gap of the semiconductor (trap depth), S is the escape frequency factor ($10^9\ \mathrm{s}^{-1}$), k is Boltzmann's constant and T is the absolute temperature.

Due to the multiexponential nature of the laser-induced photoluminescence decay curve, there are trapping levels at different depths. In an ideal case of a uniform distribution, one can assume an equal number of traps at all depths. However, in most of the cases, the distribution of traps at different depths is not uniform and is given by

$$I = I_0 t^{-b}, \tag{3}$$

where b is called the decay constant, a deciding factor for the distribution of trap states.

2.4 *X-ray diffraction studies*

Bulk crystals of zinc oxide doped with killer impurities (Fe/Co/Ni) have been studied using the X-ray diffraction (XRD) pattern. XRD data for structural characterization of the various prepared samples of ZnO were collected on an X-ray diffractometer (PW1710) using Cu K_α radiation.

3 Results

Laser-induced photoluminescence decay curves, shown in Fig. 1b, were observed using the experimental set-up described in Fig. 1a and used to simulate the lifetime, trap-depth and decay-constant values which are given in Table 1. With the addition of killer impurities the lifetime values are varying from 3.98 μs to 36.56 μs, the trap-depth values are ranging between 0.215 eV and 0.273 eV and the decay-constant values lie between 0.50 and 0.68. A general trend of decrease in lifetime and trap-depth values is observed with increase in concentration of killer impurities in ZnO phosphors. A few exceptions such as ZnO:Fe (0.5%), ZnO:Ni (0.5%) are not obeying the decreasing trend and their lifetime and trap-depth values are highest amongst the Fe- and Ni-doped ZnO phosphors, respectively. A mixed trend in decay-constant values is observed with different impurities and their concentrations. Figure 2 represents the graphs showing the trends of the lifetime values (Fig. 2a) and trap-depth values (Fig. 2b) with killer-ion concentrations. Figure 3 represents the X-ray diffraction patterns for the ZnO:Co, ZnO:Fe and ZnO:Ni phosphors indicated by curves (a), (b) and (c), respectively. Diffraction peaks corresponding to the planes ⟨100⟩, ⟨002⟩ and ⟨101⟩, obtained from X-ray diffraction data, are consistent with the JCPDS data of ZnO. Table 2 represents the XRD data (plane, 2 theta values, d-spacing and relative intensity) of the doped ZnO phosphors.

4 Discussion

Decay curves are multiexponential in nature from where lifetime, trap-depth and decay-constant values have been peeled off. The decreasing trends of lifetime and trap-depth values are attributed to the fact that the effect of killer impurities is more prominent at higher concentrations and indicates the presence of shallow trapping states at particular values of killer concentrations. The excitation of shallow trapping states in doped ZnO phosphors is mainly due to use of a high peak power and short pulse width UV nitrogen laser; otherwise they are impossible to excite with ordinary UV lamps. Fe, Co or Ni act as efficient carrier trap-

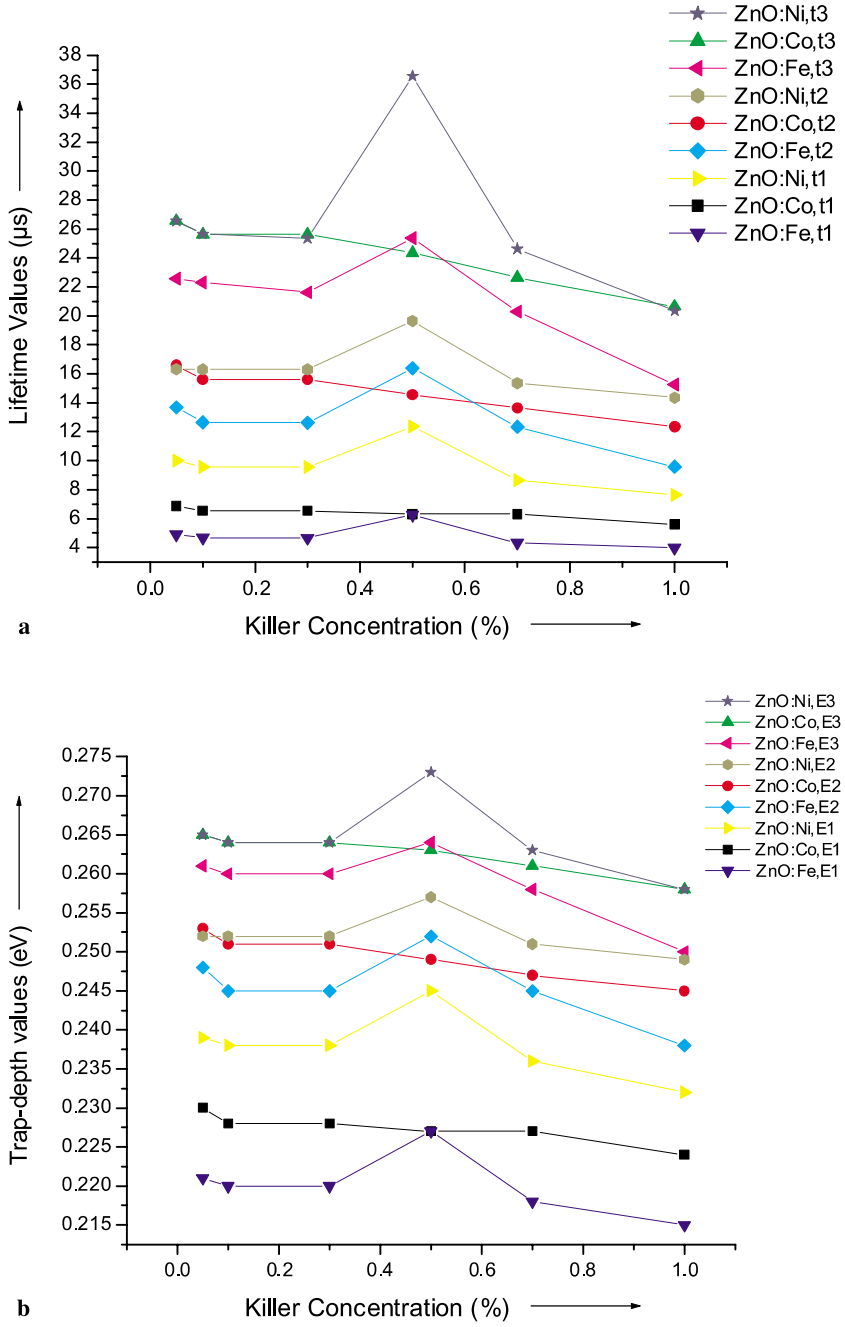

FIGURE 2 Graphs showing the trends of (**a**) lifetime values with killer (Fe, Co, Ni) concentrations and (**b**) trap-depth values with killer (Fe, Co, Ni) concentrations

ping and recombination centers, and the increase of killer concentration decreases the lifetime values. Besides the trapping process involving killer impurities, the luminescence is a more complicated process due to uncontrolled impurities and surface defects. Decay-constant values are showing a mixed effect with change in impurity concentrations. The value of the decay constant of 0.68 corresponding to ZnO:Ni (1%) is highest among all the doped ZnO phosphors. This means that the traps are more uniform at this particular concentration. A very simple and general model is proposed for the luminescence of killer-doped ZnO phosphors and is shown in Fig. 4. This energy-band diagram of a semiconductor compound represents that the killer impurity levels are lying in the forbidden band gap, responsible for luminescence and fast decay rates. The X-ray diffraction pattern observed of the ZnO:Co (0.5%) ZnO:Fe (0.5%) and ZnO:Ni (0.5%) show highly crystalline wurtzite structure of phosphors. Phase transitions or any other phase due to killer impurities were not observed in XRD studies, but minor changes in *d*-spacing corresponding to respective planes were observed. No separate phase formation in doped ZnO phosphors, observed from XRD patterns, indicates that the dopant charge carriers are contributing to the luminescence. However, an increase in concentration values, beyond a certain limit, can lead to formation of a separate phase. Dopant concentration values were set at minimum levels so as not to form a separate phase but to contribute only as charge carriers.

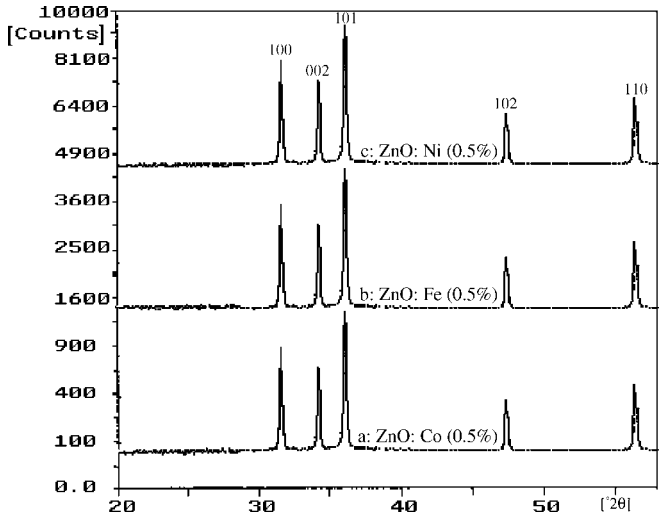

FIGURE 3 XRD of doped ZnO phosphors. Curve (a) corresponds to ZnO:Co (0.5%), (b) corresponds to ZnO:Fe (0.5%) and (c) corresponds to ZnO:Ni (0.5%)

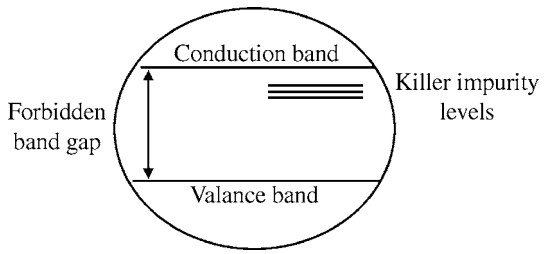

FIGURE 4 Energy-band diagram of semiconductor compound doped with killer impurities

ZnO phosphor: killer impurity	Plane	2 theta value	*d*-value	Relative intensity
ZnO:Co (0.5%)	100	31.785	2.8130	60.7
	002	34.440	2.6020	43.4
	101	36.265	2.4751	100.0
	102	47.550	1.9107	20.8
	110	56.600	1.6248	31.4
ZnO:Fe (0.5%)	100	31.605	2.8286	60.4
	002	34.255	2.6156	42.9
	101	36.095	2.4864	100.0
	102	47.380	1.9172	20.7
	110	56.445	1.6289	30.4
ZnO:Ni (0.5%)	100	31.620	2.8273	59.0
	002	34.270	2.6145	42.5
	101	36.110	2.4854	100.0
	102	47.390	1.9168	20.2
	110	56.460	1.6285	29.3

TABLE 2 X-ray diffraction data for doped ZnO phosphors

5 Conclusions

A nitrogen laser has been used to excite the short-lived trapping states present within the forbidden band gap of a semiconductor compound. From multiexponential curves, lifetime, trap-depth and decay-constant values are observed. The change in lifetime, trap-depth and decay-constant values may lie in fact that (1) the killer impurities are modifying the levels of the host ZnO semiconductor compound, (2) the levels are introduced by the killer ions in the host material or (3) there may be some defects present within or at the surface of the host material. The most favorable condition from the decreasing trends of lifetime and trap-depth values is that the killer impurity has introduced its own levels. Selective excitation of the levels can make ZnO an active medium for laser oscillations. The improved efficiency of these fast transitions in the doped semiconductor compound makes it a very suitable material for the information storage and opto-electronics industry.

ACKNOWLEDGEMENTS This work has been supported by the University Grants Commission, New Delhi, India (Project No. 31-19/2005). The authors also acknowledge Mr. Jagtar Singh, RSIC Panjab University, Chandigarh, India for providing XRD patterns.

REFERENCES

1 K. Ueda, H. Tabat, T. Kawai, Appl. Phys. Lett. **79**, 988 (2001)
2 K. Sato, H.K. Yoshida, Semicond. Sci. Technol. **17**, 376 (2002)
3 C. Boemare, T. Monteiro, J.G. Guilherme, E. Alves, Physica B **308**, 985 (2001)
4 K. Vanheusden, W.L. Warren, C.H. Seager, D.R. Tallant, J.A. Voigt, B.E. Gnade, J. Appl. Phys. **79**, 7983 (2001)
5 D.C. Look, D.C. Reynolds, C.W. Litton, R.L. Jones, D.B. Eason, G. Cantwell, Appl. Phys. Lett. **81**, 1830 (2002)
6 E. Alves, K. Lorentz, R. Vianden, C. Boemare, M.J. Soares, T. Monteiro, Mod. Phys. Lett. B **28**, 1281 (2001)
7 K. Thonke, T. Gurber, N. Teofilov, R. Schonefelder, A. Waag, R. Sauer, Physica B **308**, 945 (2001)
8 P. Dahan, V. Fleurov, P. Thurian, R. Heitz, A. Hoffmann, I. Broser, J. Phys. **10**, 2007 (1998)
9 R. Dingle, Phys. Rev. Lett. **23**, 579 (1969)
10 T. Monteiro, C. Boemare, M.J. Soares, E. Rita, E. Alves, J. Appl. Phys. **93**, 8995 (2003)
11 N.Y. Garces, L. Wang, L. Bai, N.C. Giles, L.E. Halliburton, G. Cantwell, Appl. Phys. Lett. **81**, 622 (2002)
12 G.A. Slack, B.M. O'Meara, Phys. Rev. **163**, 187 (1967)
13 J.V. Smith, *Feldspar Minerals*, vol. 1, *Crystal Structure and Physical Properties* (Springer, Heidelberg, 1974), p. 558
14 J.E. Greake, G. Walker, *Infrared and Raman Spectroscopy of Lunar and Terrestrial Minerals* (Academic Press, New York, 1975), p. 73
15 L.F. Johnson, R.E. Dietz, H.J. Guggenheim, Appl. Phys. Lett. **5**, 21 (1964)
16 J.B. Gruber, A. Kennedy, B. Zandi, J.A. Hutchinson, Proc. SPIE **3928**, 142 (2000)
17 J.B. Gruber, T.A. Reynolds, T. Alekel, D.K. Sardar, B. Zandi, D.A. Keszler, Phys. Rev. B **64**, 45 111 (2001)
18 C. Bauer, G. Boschloo, E. Mukhtar, A. Hagfeldt, Chem. Phys. Lett. **387**, 176 (2004)
19 P.V. Kamat, B. Patrick, J. Phys. Chem. **96**, 6829 (1992)
20 H.C. Zhang, Acta Phys. Sin. **49**, 1171 (2000)
21 H.S. Bhatti, R. Sharma, N.K. Verma, S.R. Vadera, K. Manzoor, J. Phys. D **39**, 1754 (2006)
22 H.S. Bhatti, A. Gupta, N.K. Verma, S. Kumar, J. Mater. Sci. Mater. Electron. **17**, 281 (2006)
23 A. Gupta, H.S. Bhatti, D. Kumar, N.K. Verma, R.P. Tandon, Dig. J. Nanomater. Biostruct. **1**, 1 (2006)
24 H.S. Bhatti, R. Sharma, N.K. Verma, Physica B **382**, 38 (2006)